Journal of Crystal Growth 312 (2010) 2012–2018

Contents lists available at ScienceDirect

Journal of Crystal Growth

journal homepage: www.elsevier.com/locate/jcrysgro

Comparative study of ZnO thin film and nanopillar growth on YSZ(1 1 1) and sapphire (0 0 0 1) substrates by pulsed laser deposition

Himanshu Verma, Devajyoti Mukherjee, Sarath Witanachchi, Pritish Mukherjee, Matthias Batzill *

Department of Physics, University of South Florida, Tampa, FL 33620, USA

ARTICLE INFO

Article history:
Received 23 September 2009
Received in revised form
23 February 2010
Accepted 19 March 2010
communicated by J.B. Mullin
Available online 1 April 2010

Keywords:
A1. Substrates
A1. Nanostructures
A1. Morphological stability
A1. Surface structure
A3. Laser epitaxy
B1. Oxides

ABSTRACT

The growth of ZnO films by pulsed laser deposition was systematically studied on three different substrates, namely YSZ(1 1 1), Al_2O_3(0 0 0 1), and Si(1 0 0). The dependence of the film morphology on oxygen background pressure and substrate temperature was investigated. A strong dependence of the ZnO morphology on all three growth parameters was found allowing for tuning the microscopic structure of ZnO from contiguous film to a columnar growth, and to perfectly aligned nanopillars.

1. Introduction

Zinc oxide (ZnO) is a material with applications for UV-photoelectronic devices due to its large exciton binding energy of 60 meV and direct band gap of 3.4 eV [1–3]. In addition it finds applications as transparent conducting oxide, [4] gas sensor, [5] and photocatalyst [6,7] or electrodes for photoelectrochemical cells [8–10]. By appropriate doping the ferroelectric and ferromagnetic properties of ZnO can be altered and produces potentially important materials such as room temperature ferromagnetic semiconductors [11]. In addition a variety of nanostructured ZnO morphologies have been synthesized by solution or vapor transport methods with and without the use of metal catalysts [12–14]. Recently, it has been shown that aligned ZnO-nanowires can also be grown by pulsed laser deposition (PLD) on sapphire substrates without metal catalysts [15–18]. PLD has the advantage of transferring the composition of a target to a film and thus provides a convenient way of growing complex, many-component materials and for growing films with defined dopant concentration. Therefore, growth of ZnO-nanowires by PLD has the potential advantage of enabling control of the nanowire properties by doping. In this communication we concentrate on the microstructure of pure ZnO films and investigate the role of the substrates and other growth parameters on film morphologies.

ZnO films have a preference to grow with a *c*-axis orientation [19]. In addition ZnO films with a defined crystallographic relationship with the substrate have been grown successfully by various deposition methods on *c*-plane oriented sapphire, i.e. α-Al_2O_3(0 0 0 1), and also on yttria stabilized zirconia YSZ (1 1 1) [20]. It appears that the same hexagonal symmetry of the substrates' surface unit cell compared to the *c*-plane of ZnO, i.e. the (0 0 0 1) crystallographic plane is sufficient to cause the epitaxial relationship between substrate and film. This crystallographic relationship between the substrates and ZnO(0 0 0 1) is illustrated in Fig. 1. The lattice mismatch between the substrates and ZnO is large with 8% and 26% for YSZ and sapphire, respectively. This large misfit prohibits a pseudomorphic growth and consequently results in defects and film imperfections that affect their properties.

Up to now, most ZnO thin films have been grown on sapphire and only a few studies have been reported on YSZ [21–23]. However, since YSZ has a more favorable lattice match with ZnO compared to sapphire we investigate if better film and surface properties of ZnO films can be obtained on YSZ. To this end we compare the growth of ZnO films and nanostructures on Si (with native oxide layer), Al_2O_3(0 0 0 1), and YSZ(1 1 1) substrates as a function of growth temperature and pressure.

With increasing pressure (>300 mTorr) and higher substrate temperatures (>500 °C) a transition from contiguous ZnO film

* Corresponding author.
E-mail address: mbatzill@cas.usf.edu (M. Batzill).

0022-0248/$ - see front matter © 2010 Elsevier B.V. All rights reserved.
doi:10.1016/j.jcrysgro.2010.03.030

growth to a columnar and finally to the formation of vertically aligned nanopillars is observed on all substrates. This is in agreement with previous studies. It was also noted that at very high pressures (>1 Torr) the nanopillars seem to grow with larger diameter while at intermediate pressures (300–500 mTorr) nanopillars with diameters as small as 50 nm were obtained. The transition from film growth to nanopillar formation at a threshold background pressure has been proposed to be a consequence of the thermalization of the ablation plume and thus suggesting that a lower surface mobility of the deposited species is required for nanopillar formation. On the other hand, it has also been reported that the nanopillar diameter decreases with sample temperature at constant pressure, indicating that higher surface mobility decreases the nanopillar diameter [17]. In this communication we show that the substrate also effects the growth mode and we find that alumina is best suited for the formation of well ordered nanopillars while YSZ(1 1 1) is the preferred substrate for contiguous ZnO films.

2. Experimental methods

ZnO films were grown on YSZ(1 1 1), Al_2O_3(0 0 0 1), and Si(1 0 0) (with oxide layer) by PLD at various sample temperatures and oxygen background pressures. The substrates were cleaned ultrasonically with acetone, methanol, and DI water prior to mounting in the PLD chamber. The base pressure in the PLD chamber was 10^{-6} Torr and the background pressure was adjusted by leaking high purity oxygen gas into the chamber. The ZnO target was ablated with a KrF excimer laser ($\lambda=248$ nm, 10 Hz, 154 mJ/pulse, and energy density of 2 J/cm^2). The target to the substrate distance was kept constant at 6 cm. All the films were grown for the same amount of deposition time using 20,000 laser pulses at a repetition rate of 10 Hz. Films grown under low ambient pressure of 10 mT had a nominal thickness of ~450 nm for substrate temperatures of 300–450 °C with a slight drop in the thickness at substrate temperature of 600 °C to 400 nm. However the films grown under a high ambient pressure of 100 and 500 mT were over 1 μm thick with the thickness increasing with higher background pressure irrespective of the substrate temperature. The film thickness was same irrespective of the type of substrate used.

After removing the samples from the growth chamber the samples were characterized by X-ray diffraction (XRD), scanning electron microscopy (SEM) and for reasonably smooth films, by atomic force microscopy (AFM). SEM images were also acquired in a cross-sectional view by cleaving of the samples.

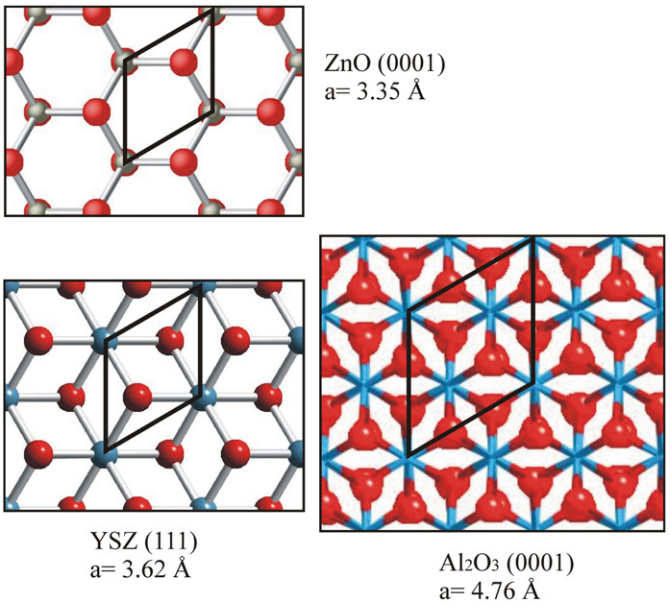

Fig. 1. Ball-and-stick models of surfaces of ZnO(0 0 0 1), YSZ(1 1 1), and Al_2O_3(0 0 0 1). The hexagonal surface unit cells and their lattice constants are shown. All models are drawn to scale.

3. Results

The structural properties of ZnO films were assessed as a function of background pressure and sample temperature for the different substrates. XRD indicates that for all growth conditions only *c*-axis oriented ZnO films and nanowires were obtained on Al_2O_3(0 0 0 1) and YSZ(1 1 1) substrates. For different growth conditions, the full-width at half-maximum (FWHM) of the rocking curves for the ZnO(0 0 2) peak showed, however, variation with the growth parameters. Table 1 summarizes the FWHM for the different films. These numbers may be compared to the reference value measured on a single crystal ZnO wafer of 0.06°. The higher FWHM value of the films compared to the single crystal clearly indicates that the film consists of grains with small vertical misalignments. On both Al_2O_3 and YSZ the FWHM is decreasing with increasing sample temperature with the largest improvement observed between 300 and 450 °C. For identical growth conditions the FWHM of the ZnO rocking curve is always smaller on YSZ than alumina substrates indicating a better vertical orientation and/or larger grain sizes on YSZ.

Further surface structural analysis was performed by SEM and AFM. RMS roughness, for films that were smooth enough to allow for reasonable AFM characterization, is also summarized in Table 1. It is interesting to note that there is a trend for films with *smaller* FWHM in the rocking curves, i.e. better *c*-axis alignment of grains, to have a generally *larger* surface RMS roughness measured in AFM. Such a correlation could be a consequence of ZnO to grow in a columnar fashion which allows a surface with smaller, misaligned grains to be smoother than a

Table 1
Comparison of ZnO(0 0 2) rocking curves and RMS roughness for different substrates and growth conditions.

Growth condition ↓ Sample →	Rocking curve FWHM Al_2O_3-0001	Rocking curve FWHM YSZ-111	Rocking curve FWHM Si-100	RMS roughness (in nm) Al_2O_3-0001	RMS roughness (in nm) YSZ-111	RMS roughness (in nm) Si-100
300 °C, 100 mT	2.04°	1.72°	2.35°	24.0	42.1	19.7
450 °C, 10 mT	0.46°	0.29°	1.38°	91.8	90.0	90.1
450 °C, 100 mT	0.67°	0.33°	2.83°	24.9	15.2	41.4
450 °C, 500 mT	0.57°	0.36°	–	Too rough	Too rough	–
600 °C, 10 mT	0.46°	0.26°	2.14°	57.5	39.3	–
600 °C, 100 mT	0.40°	0.20°	8.51°	Too rough	Too rough	–
600 °C, 500 mT	0.32°	0.21°	–	Too rough	Too rough	–

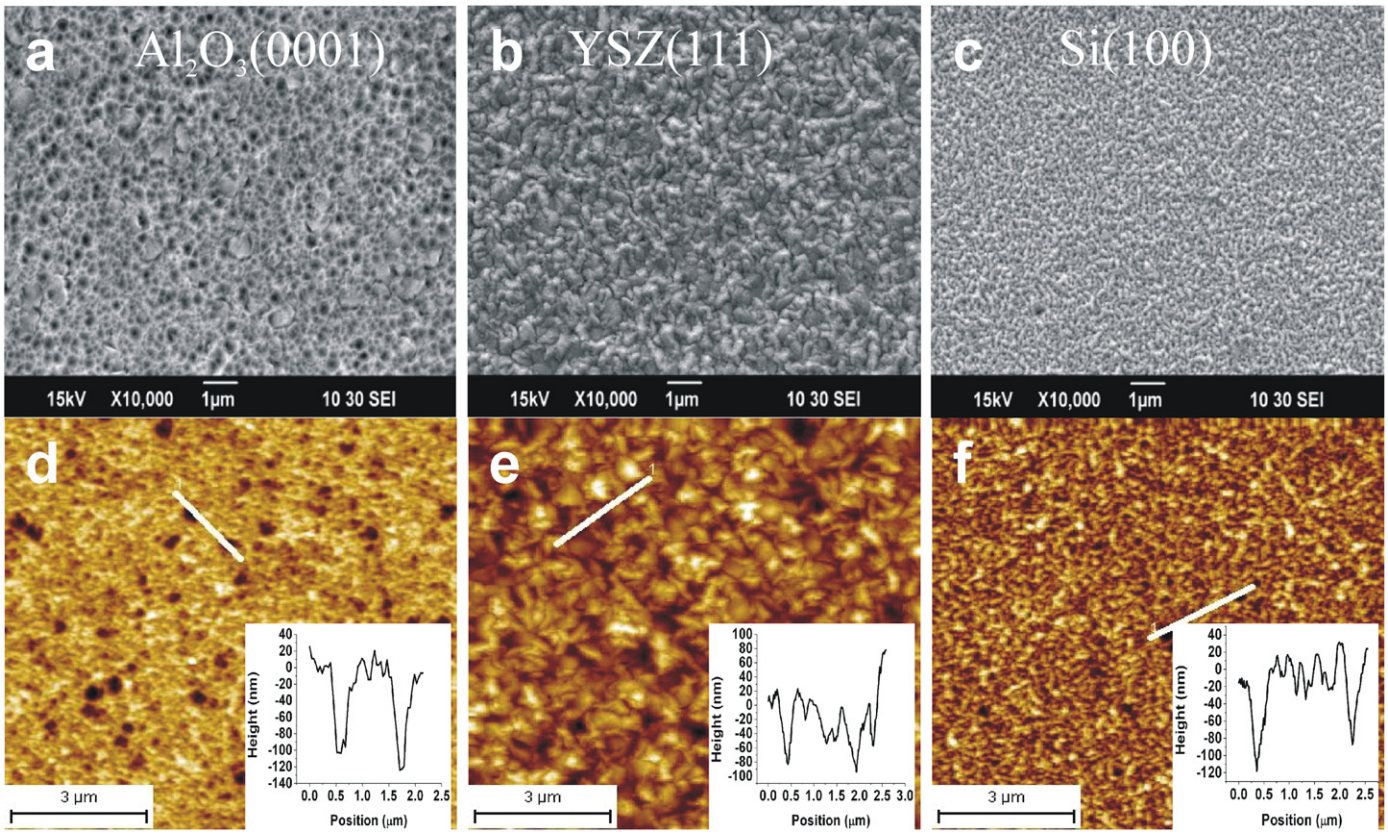

Fig. 2. ZnO film at 300 °C, 100 mT: (a) SEM on Al_2O_3(0 0 0 1), (b) SEM on YSZ(1 1 1), (c) SEM on Si(1 0 0), (d) AFM on Al_2O_3(0 0 0 1), (e) AFM on YSZ(1 1 1), and (f) AFM on Si(1 0 0). The graphs in the inset show line profile of the AFM images.

surface with better aligned but larger grains that grow independently of each other.

The surface morphologies of ZnO films characterized with AFM and SEM on the different substrates are discussed in the following. Fig. 2 shows films prepared at a substrate temperature of 300 °C with an oxygen background pressure of 100 mTorr. Under these low temperature conditions a high value in the FWHM in the rocking curve suggests poor alignment of crystals and this is also reflected in the surface micrographs in Fig. 2. The largest crystallites are observed on YSZ(1 1 1) followed by Al_2O_3(0 0 0 1) and Si(1 0 0).

Increasing the temperature to 450 °C and reducing the pressure allows better ordering of the films, which results in larger crystallites as is apparent from the micrographs shown in Fig. 3. The surface morphologies of ZnO films grown on Al_2O_3 and YSZ are very similar under these conditions, exhibiting large grains. The surface morphology of ZnO on Si is different, exhibiting an interconnected 'ridge' structure with 100 nm deep holes. Keeping the temperature at 450 °C but increasing the pressure to 100 mTorr causes the formation of, what appears to be, smaller grains on both Al_2O_3 and YSZ, which also causes a smoother surface. This is shown in Fig. 4. Under these conditions the surface structure is again very similar on all three substrates. Increasing the pressure further causes the clear formation of columnar ZnO growth which is evident from the SEM micrographs shown in Fig. 5.

Figs. 6–8 show micrographs of samples grown at 600 °C and at 10, 100, and 500 mTorr, respectively. Under these high temperature conditions a columnar growth is observed that transforms to a nano-column growth of separated structures at high pressures. Clear differences in the film morphologies are observed for the different substrates. At 100 mTorr pressure the film on Al_2O_3(0 0 0 1) show dense ZnO columns of ~200 nm width, while on YSZ(1 1 1) large grains with hexagonal shape and micrometer width are observed. Increasing the pressure to 500 mTorr results in the formation of separated and aligned nano-columns of ~50–100 nm width on Al_2O_3(0 0 0 1). On YSZ(1 1 1) also columnar growth is observed, however, the column widths is a little larger in the range of 100–150 nm. The top-view in SEM suggests that these columns are more densely packed on YSZ(1 1 1) and the columns cluster together to form structures that appear like meandering 'worms'. In addition to these narrow wires some larger hexagonal grains, reminiscent of those observed at 100 mTorr, are observed dispersed within the nano-columns. On Si(1 0 0) the film is very different. Although we still observe growth of separated grains, the grains are much larger (micrometer size) and no orientational alignment of the grains are observed indicating the importance of the substrate for determining the growth direction of the ZnO columns.

4. Discussion

The film morphologies of ZnO grown by PLD are strongly dependent on the growth parameters (background pressure and substrate temperature). Only considering the substrates with hexagonal symmetry, i.e. YSZ(1 1 1) and Al_2O_3(0 0 0 1), we may distinguish four growth regimes.

The first growth regime is at low temperatures (below ~300 °C) and the ZnO films exhibit poor *c*-axis alignment evident from the broad rocking curves. The surface RMS roughness is, however, comparable to their lowest values achieved for all the growth parameters. Obviously, at low sample temperatures thermal activation is not sufficient to find a low energy alignment of the crystallites in the film.

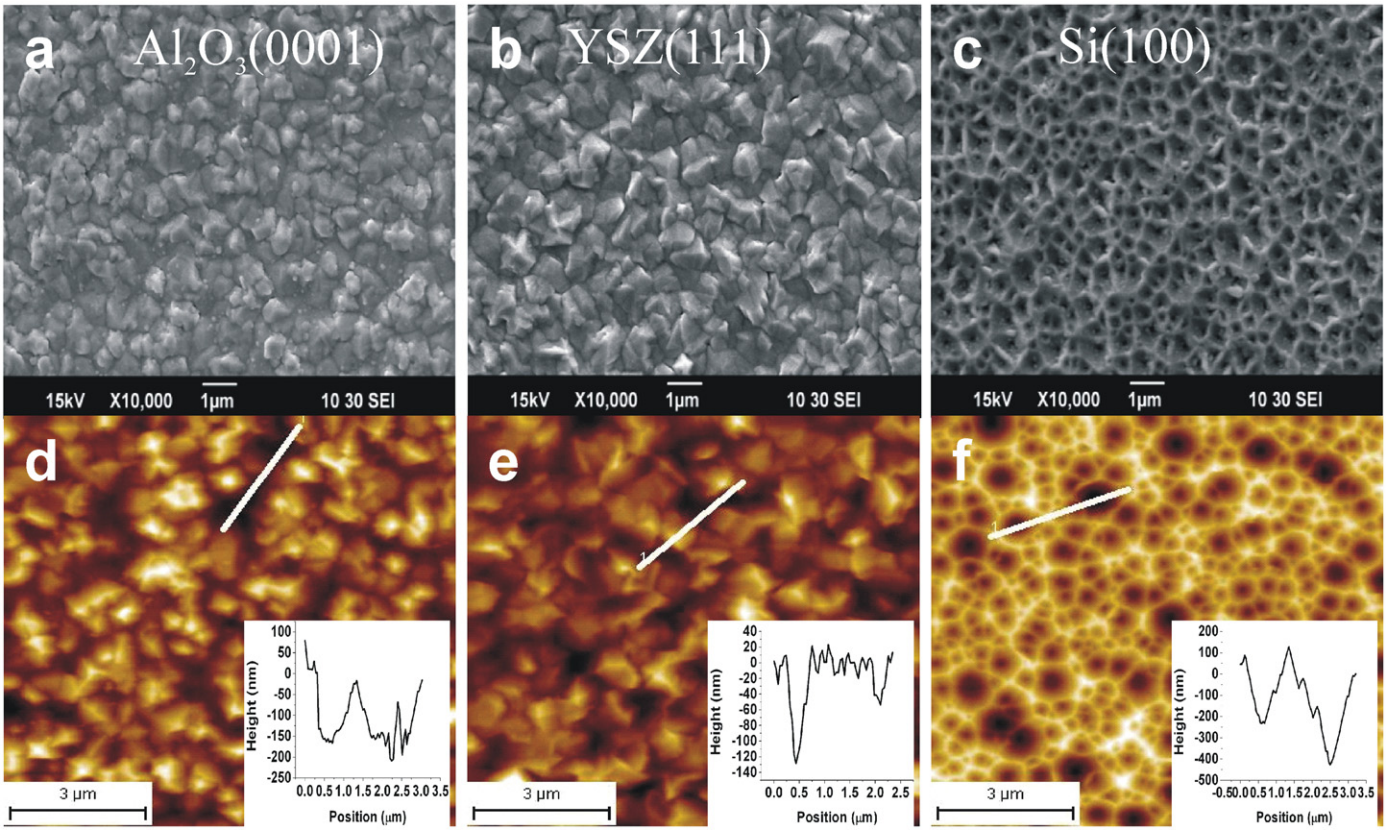

Fig. 3. ZnO film at 450 °C, 10 mT: (a) SEM on Al_2O_3(0 0 0 1), (b) SEM on YSZ(1 1 1), (c) SEM on Si(1 0 0), (d) AFM on Al2O3(0 0 0 1), (e) AFM on YSZ(1 1 1), and (f) AFM on Si(1 0 0). The graphs in the inset show line profiles of the AFM images.

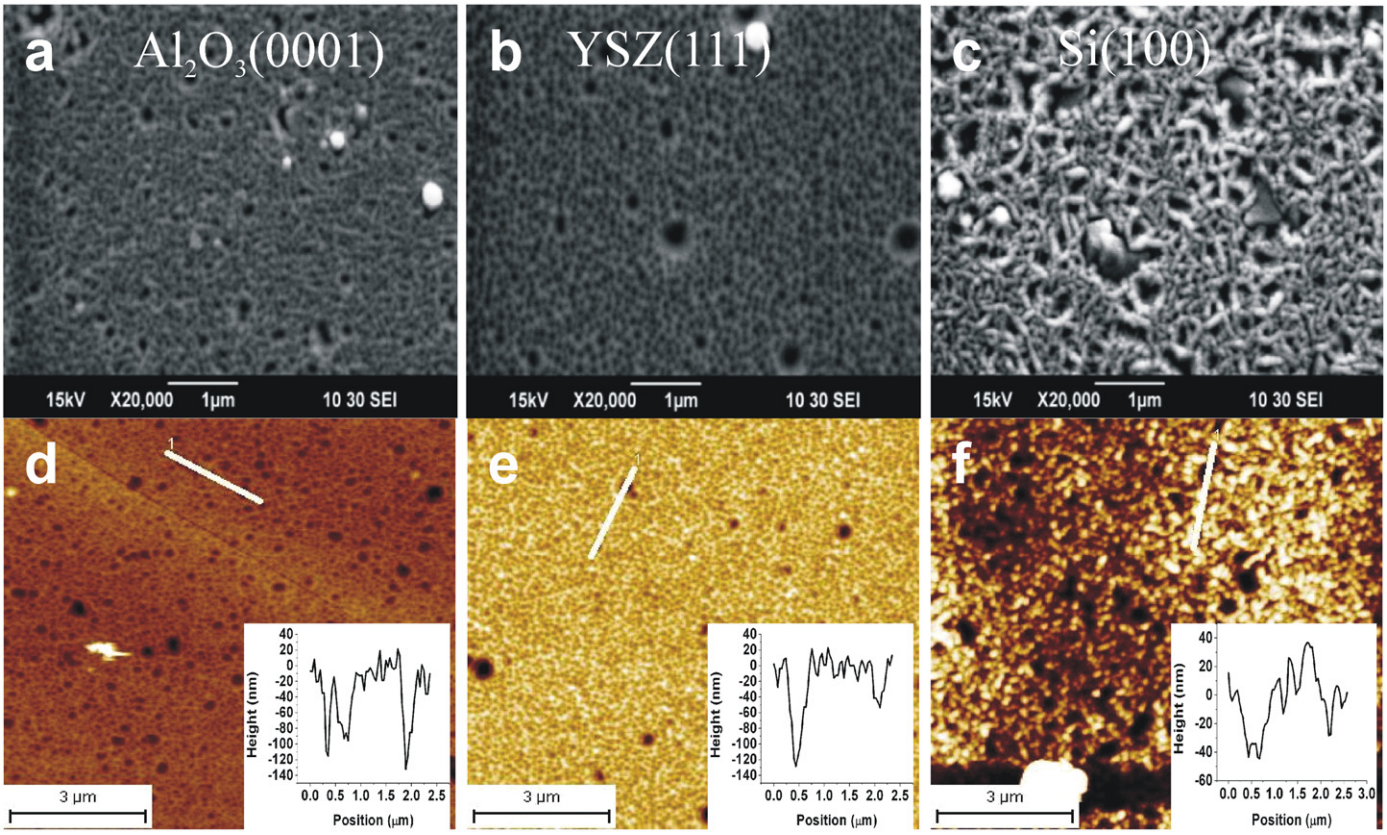

Fig. 4. ZnO film at 450 °C, 100 mT: (a) SEM on Al_2O_3(0 0 0 1), (b) SEM on YSZ(1 1 1), (c) SEM on Si(1 0 0), (d) AFM on Al_2O_3(0 0 0 1), (e) AFM on YSZ(1 1 1), and (f) AFM on Si(1 0 0). The graphs in the inset show line profile of the AFM images.

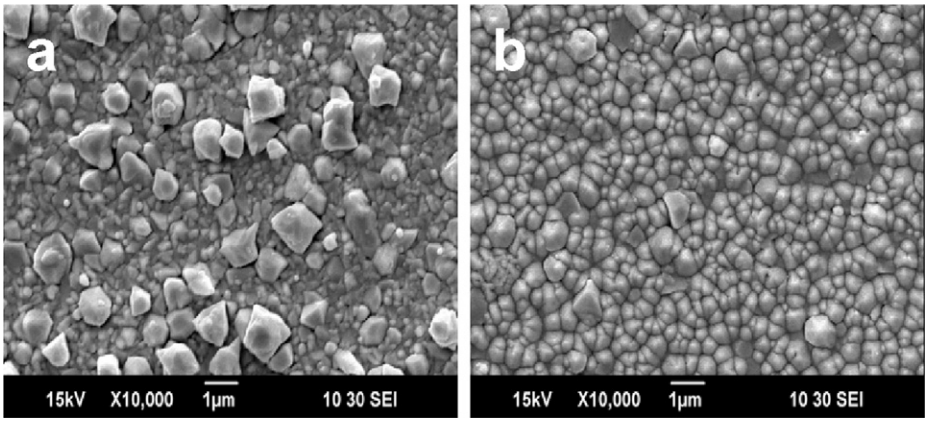

Fig. 5. ZnO film at 450 °C, 500 mT: (a) SEM on Al_2O_3(0 0 0 1) and (b) SEM on YSZ(1 1 1).

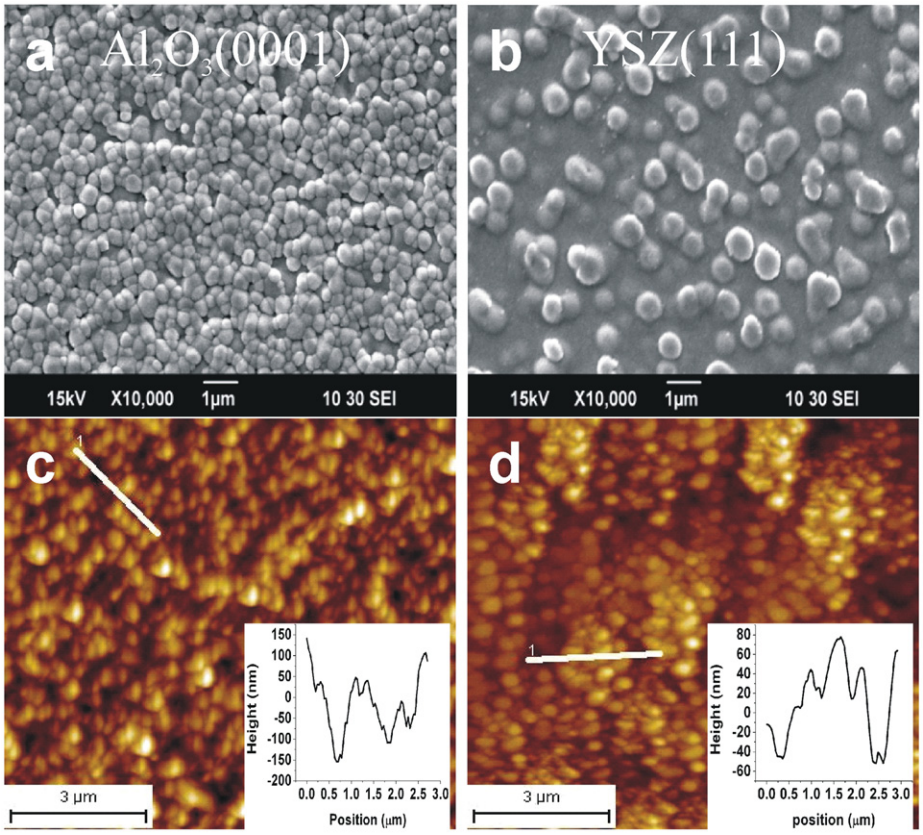

Fig. 6. ZnO film at 600 °C, 10 mT: (a) SEM on Al_2O_3(0 0 0 1), (b) SEM on YSZ(1 1 1), (c) AFM on Al2O3(0 0 0 1), and (d) AFM on YSZ(1 1 1). The graphs in the inset show line profile of the AFM images.

In the second growth regime this thermal limitation is lifted and FWHM of the rocking curves is reduced significantly and the surface is smooth without indications of *c*-axis aligned columns. This growth regime is around ~450 °C and pressures at or below 100 mTorr. The surface topography differs between films grown with different background pressures at 450 °C. At 10 mTorr micrometer sized individual crystallites are discernable in SEM images, which give rise to a fairly high surface RMS roughness. At higher pressures (100 mTorr) the surface is less rough and the FWHM in rocking curves is slightly increased compared to films grown at 10 mTorr. This difference in the film morphologies at constant temperature but different background pressure can be explained by a more efficient thermalization of the ablation plume and consequently lower mobility of ad-atoms at elevated pressures. Higher mobility gives rise to the growth of larger crystallites with low-energy facets exposed at the surface. Up to this point the films are continuous, which is also evident from frequently observed cracks in the film attributed to differential thermal expansion of the film and substrate material. Such cracks can only occur if the film is continuous.

At higher background pressure (500 mTorr at 450 °C sample temperature) or higher sample temperature (600 °C at 10–100 mTorr) the ZnO films grow in columnar grains, with grain boundaries intersecting the ZnO film from the substrate to the film surface normal to the film, i.e. along the *c*-axis. From our cross-sectional SEM it is not possible to tell if these columnar grains are already separated or if these films could be still considered as continuous. It appears that higher temperature and higher pressure have similar effects on the film morphology. This is surprising since these two parameters

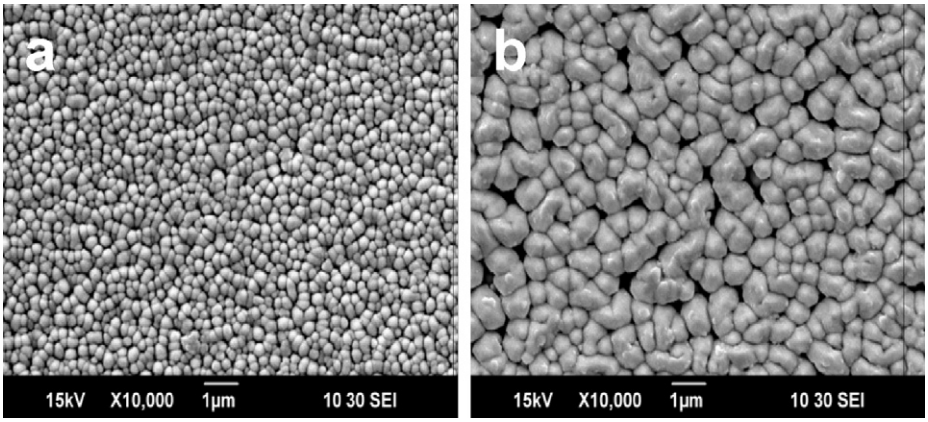

Fig. 7. ZnO film at 600 °C, 100 mT: (a) SEM on Al_2O_3(0 0 0 1) and (b) SEM on YSZ(1 1 1).

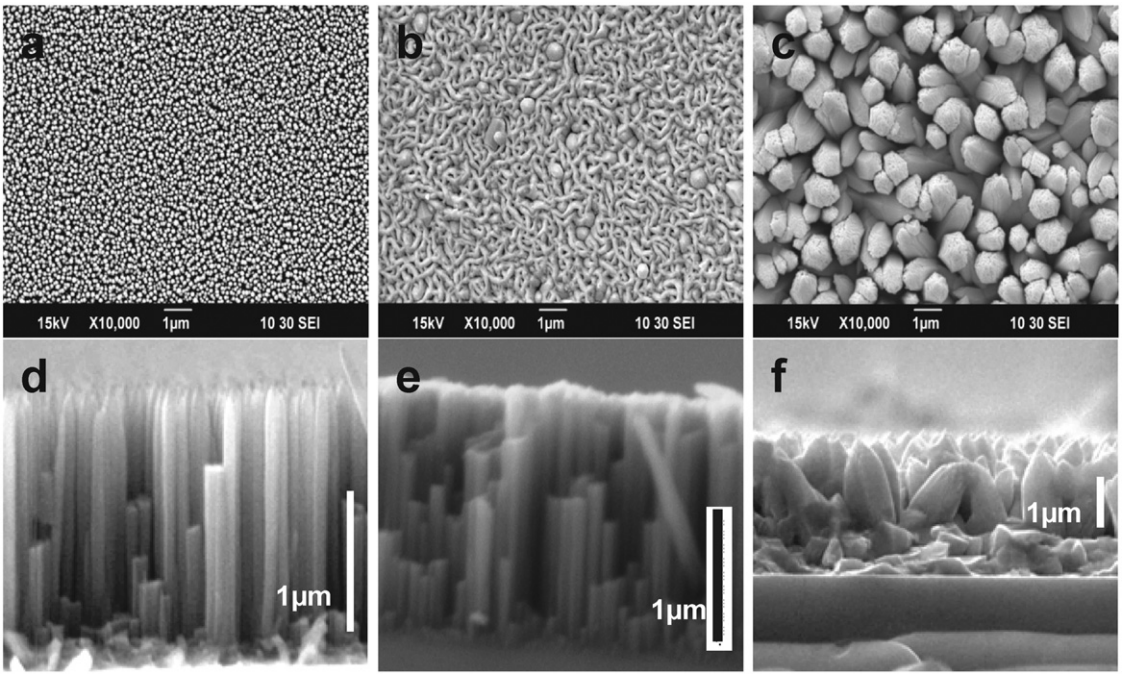

Fig. 8. ZnO film at 600 °C, 500 mT: (a) SEM on Al_2O_3(0 0 0 1), (b) SEM on YSZ(1 1 1), (c) SEM on Si(1 0 0), (d) cross-section SEM on Al_2O_3 (0 0 0 1), (e) cross-section SEM on YSZ(1 1 1), and (f) cross-section SEM on Si(1 0 0).

should counteract each other, i.e. a higher pressure decreases the energy of the atoms in the ablation plume while higher temperature increases mobility of surface species. On the other hand, higher mobility of surface species is often observed in the presence of oxygen and this may compensate for the decreased kinetic energy of the atoms in the plume at higher oxygen pressures.

Finally, at 600 °C and pressures of 100 mTorr or higher, free-standing ZnO columns or 'nano-pillars' are observed. The excellent *c*-axis alignment on alumina and YSZ is evident from the low FWHM of the rocking curve. Isolated grain-growth is also observed on silicon wafers under these conditions, however, as expected only very poor alignment is observed demonstrating that a substrate with similar symmetry to that of the ZnO lattice is needed to orient the growth.

5. Conclusion

In terms of growth parameters it appears that with higher pressure and temperatures the growth mode in PLD converts from a continuous film to a columnar growth that eventually results in the growth of free-standing micro(nano)-pillars. The materials transport and atomic processes that cause such a dramatic change in the growth are currently not well understood and need further investigation.

Compared to the growth parameters the choice of substrate, i.e. Al_2O_3(0 0 0 1) or YSZ(1 1 1), affects the film morphology to a lesser extent. However, some clear trends are noteworthy. The FWHM of the rocking curves has been always less for YSZ(1 1 1) substrates compared to Al_2O_3(0 0 0 1) substrates for otherwise identical growth conditions. This indicates that the orientational *c*-axis alignment of the ZnO film is better on YSZ than on sapphire. On the other hand, growth of nanopillars at elevated temperatures and pressures resulted in more uniform surface morphologies on sapphire than on YSZ. These differences may be associated with the different lattice mismatch between the two substrates. Therefore YSZ(1 1 1) is a better substrate for the growth of *c*-axis oriented films while Al_2O_3(0 0 0 1) makes a better substrate for separated nanopillar growth.

Acknowledgment

This material is based upon work supported by the National Science Foundation under Grant no. CHE-0840547 and Department of Defense Grant no. W81XWH-07-1-0708.

References

[1] S. Singh, P. Thiyagarajan, K.M. Kant, D. Anita, S. Thirupathiah, N. Rama, B. Tiwari, M. Kottaisamy, M.S.R. Rao, J. Phys. D Appl. Phys. 40 (2007) 6312.
[2] C. Klingshirn, Phys. Status Solidi B 224 (2007) 3027.
[3] U. Ozgur, Y.I. Alivov, C. Liu, A. Teke, M.A. Reshchikov, S. Dogan, V. Ayrutin, S.J. Cho, H. Morkoc, J. Appl. Phys. 98 (2005) 041301.
[4] M. Batzill, U. Diebold, Prog. Surf. Sci. 79 (2005) 47.
[5] G. Sberveglieri, Sensors Actuators B 23 (1995) 103.
[6] N. Kislov, J. Lahiri, H. Verma, D.Y. Goswami, E. Stefanakos, M. Batzill, Langmuir 25 (2009) 3310.
[7] F. Xu, Z.-Y. Yuan, G.-H. Du, T.-Z. Ren, C. Bouvy, M. Halasa, B.-L. Su, Nanotechnology 17 (2006) 588.
[8] H.E. Unalan, D. Wei, K. Suzuki, S. Dalal, P. Hiralal, H. Matsumoto, S. Imaizumi, M. Minagawa, A. Tanioka, A.J. Flewitt, W.I. Milne, G.A.J. Amaratunga1, Appl. Phys. Lett. 93 (2008) 133116.
[9] H.H. Chen, A. Du Pasquier, G. Saraf, J. Zhong, Y. Lu, Semicond. Sci. Technol. 23 (2008) 045004.
[10] W.J. Lee, H. Okada, A. Wakahara, A. Yoshida, Ceram. Int. 32 (2006) 495.
[11] F. Pan, C. Song, X.J. Liu, Y.C. Yang, F. Zeng, Mater. Sci, Engineering R 62 (2008) 1.
[12] Z.L. Wang Mater, Sci. Eng. R 64 (2009) 33.
[13] X.D. Wang, J.H. Song, Z.L. Wang, J. Mater. Chem. 17 (2007) 711.
[14] Z.R. Tian, J.A. Voigt, J. Liu, B. McKenzie, M.J. McDermott, M.A. Rodriguez, H. Konishi, H. Xu, Nat. Mater. 2 (2003) 821.
[15] M. Kawakami, A.B. Hartanto, Y. Nakata, T. Okada Jpn, J. Appl. Phys. 42 (2003) L33.
[16] A.B. Hartanto, X. Ning, Y. Nakata, T. Okada, Appl. Phys. A 78 (2004) 299.
[17] L.C. Tien, S.J. Pearton, D.P. Norton, F. Ren, J. Mater. Sci. 43 (2008) 6925.
[18] D. Valerini, A.P. Caricato, M. Lomascolo, F. Romano, A. Taurino, T. Tunno, M. Martino, Appl. Phys. A 93 (2008) 729.
[19] F. Claeyssens, C.L. Freeman, N.L. Allan, Y. Sun, M.N.R. Ashfold, J.H. Harding, J. Mater. Chem. 15 (2005) 139.
[20] R. Triboulet, J. Perriere Prog, Cryst. Growth Character. Mater. 47 (2003) 65.
[21] H. Ohta, H. Tanji, M. Orita, H. Hosono, H. Kawazoe, Mater. Res. Soc. Symp. Proc. 570 (1999) 309.
[22] Y.-C. Chao, C.-W. Lin, D. J. E, Y. Wu, G. Chen, L. Chang, Y. T. Ho, M.-H. Liang, J. Cryst. Growth 298 (2007) 461.
[23] C.-W. Lin, Y.-T. Ho, L. Chang, Mater. Chem. Phys. 108 (2008) 160.